Physical Communication 3 (2010) 265–275

Contents lists available at ScienceDirect

Physical Communication

journal homepage: www.elsevier.com/locate/phycom

Full length article

Upper and lower bounds on subcarrier collision for inter-cell interference scheduler in OFDMA-based systems: Voice traffic

Serhan Yarkan [a,*], Koon Hoo Teo [b], Hüseyin Arslan [c], Jinyun Zhang [b], Khalid A. Qaraqe [d]

[a] Department of Electrical and Computer Engineering, Texas A & M University, 301 Wisenbaker Engineering Research Center, Bizzell Street, College Station, TX, 77840, United States

[b] Mitsubishi Electric Research Laboratories, 201 Broadway Cambridge, MA, 02139, United States

[c] Department of Electrical Engineering, University of South Florida, 4202 E. Fowler Avenue, ENB-118, Tampa, FL, 33620, United States

[d] Department of Electrical and Computer Engineering, Texas A & M University at Qatar, Texas A & M Engineering Building, Education City, Doha, 23874, Qatar

ARTICLE INFO

Keywords:
Bound
Collision
OFDMA
Resource
Scheduling
Subcarrier
Traffic
Voice

ABSTRACT

This study investigates upper and lower bounds on subcarrier collision for inter-cell interference (ICI) schedulers in orthogonal frequency division multiple access (OFDMA)-based wireless systems carrying voice traffic. It is shown that the amount of knowledge regarding the reserved resources in the neighboring cell plays a crucial role in the performance of ICI schedulers. Also, it is proven that the upper bound of subcarrier collision for ICI schedulers corresponds to the case which is driven by the absence of knowledge about the reserved resources in the neighboring cell. On the other hand, the lower bound of subcarrier collision for ICI schedulers corresponds to the case which is driven by the perfect knowledge about the reserved resources in the neighboring cell. Based on the lower bound analysis, a minimum expected number of collision scheduler is developed and its performance is investigated as well. Moreover, the impact of scheduling period on the performance of schedulers is examined. Numerical results are presented along with related discussions.

1. Introduction

Due to the inherent nature of wireless communications, wireless terminals are exposed to interference. There are many types of interference such as co-channel interference (CCI), adjacent channel interference (ACI), and so on. CCI has a special place among these interference types, because it affects the overall design of a wireless system. Traditional cellular systems are designed in such a way that CCI is controlled by "reusing" frequencies in farther cells at the cost of underutilization of available resources, such as in Global System for Mobile (GSM) [1,2]. Frequency reuse of one (FRO) is considered to be employed especially in next generation cellular mobile networks for overcoming the underutilization problem. FRO is a very promising approach, because it reduces the need for frequency planning which is a very expensive process. Nonetheless, FRO introduces significant CCI into the system especially for the user equipments (UEs) residing in the vicinity of cell borders [3]. CCI can be controlled by coordinating the transmission from multiple sources [4,5]. Interference coordination [6] and fully adaptive and dynamic resource allocation are some of the very powerful techniques to reduce CCI [4,5,7]. In this sense, schedulers which conduct dynamic resource allocation under the FRO regime are vital units of inter-cell interference (ICI) management process in next generation wireless networks (NGWNs) [8].

Traffic type plays a crucial role in the behavior of interference. Therefore, ICI management is investigated in

* Corresponding author. Tel.: +1 7132801987; fax: +1 9798458986.
E-mail addresses: syarkan@ece.tamu.edu (S. Yarkan), teo@merl.com (K.H. Teo), arslan@eng.usf.edu (H. Arslan), jzhang@merl.com (J. Zhang), kqaraqe@tamu.edu (K.A. Qaraqe).

1874-4907/$ – see front matter © 2010 Elsevier B.V. All rights reserved.
doi:10.1016/j.phycom.2010.05.001

Symbol list

C_c	cth cell
U_c	Set of all of the users in C_c
$\mathcal{U}_c$	Number of users in C_c
u_{cj}	jth user in C_c
$\Theta(\cdot)$	Interior/cell edge distinction operator
F	Set of all of the resources
$\mathcal{F}$	Number of resources in F
$F_c^{(I)}$	Set of reserved resources for cell edge in C_c
$\mathcal{F}_c$	Number of resources in $F_c^{(I)}$
λ_H	Decaying rate of negative exponential PDF for voice calls
μ_H	Average resource holding time for voice calls
T_c	Scheduling period for C_c
$\lambda_A^{(c)}$	Arrival rate of Poisson process for C_c
T_Δ	Minimum scheduling period
r_c	Traffic load of C_c
$\mathbf{K}$	Random variable that represents number of collisions
$\Pr\{\mathcal{E}\}$	Probability of event $\mathcal{E}$
$p(k)$	Probability of $\mathbf{K}$ taking the value k
$E\{\mathbf{K}\}$	Statistical expectation for random variable $\mathbf{K}$
$\mathfrak{U}$	Upper bound of expected number of collisions
L	Certainty level for breaking point
ϵ	Precision for breaking point $(1-L)$
k_ϵ	Breaking point of precision ϵ
H_k	Bending point
$\mathfrak{L}$	Lower bound of expected number of collisions
$r_1^{\mathfrak{L}}$	Bending point of traffic load for pilot cell
$\mathfrak{X}$	Constant part of $\mathfrak{U}$ under pilot cell approach
$\mathfrak{s}$	The percentage of the knowledge acquired by the pilot cell
n	Prolongation factor of new scheduling period for the pilot cell
$\mathfrak{S}_{\min}$	Clipped expected number of collisions value obtained when $1 < n$
r_1'	Generalized pilot cell traffic load for different $\mathfrak{s}$ and n values

the literature by considering different types of traffic under various conditions. The combined effect of propagation and voice type traffic on CCI and performance of dynamic channel allocation for orthogonal frequency division multiple access (OFDMA)-based cellular systems are investigated in [9]. In [10], performance analysis of different scheduler schemes for ICI coordination in OFDMA-based networks is given under elastic traffic. In [11], ICI is investigated from the perspective of both streaming and elastic traffic under different frequency reuse schemes through the use of several scheduler performance metrics such as mean number of collisions. In [12], non-real time Internet traffic is assessed for OFDMA/frequency division duplexing (FDD)-based schedulers under ICI by aiming at increasing the number of users limited to minimum rate requirements. Analytical approaches for the capacity of OFDMA-based systems in terms of resource collisions and their impacts for adaptive and elastic traffic types are provided in [13]. ICI under full-buffer type traffic is investigated in [14] from the perspective of coordination between cells. A simulation framework based on physical layer (PHY) and medium access control (MAC) layer interaction of five different traffic types with different scheduler schemes is developed for an OFDMA-based multi-cell system in [15]. Influence of different traffic types on system capacity along with scheduling operation is assessed from simulation perspective in [16]. A multi-input multi-output (MIMO)-based system under real-time traffic for OFDMA-based schedulers is investigated in [17].

Although there are many studies in the literature regarding different ICI conditions for different traffic types, to the best knowledge of authors, there is no analytical study which connects schedulers with a particular type of traffic by providing theoretical performance limits along with the factors influencing them. Performance limits and factors influencing them are key points to develop better schedulers for ICI management process in NGWNs. In this study, performance limits on ICI schedulers in OFDMA-based systems are derived for voice traffic based on pilot cell approach under FRO regime and factors affecting them are investigated. The contributions of this work is threefold. First, it is formally shown that the knowledge about the resource reservation of the neighboring cell plays a crucial role in upper and lower bounds for ICI schedulers. More concretely, it is shown that theoretical upper bound corresponds to the cases that are driven by the absence of knowledge (absolute uncertainty), whereas lower bound corresponds to the cases that are driven by the presence of perfect knowledge (absolute certainty).

Second, Minimum Expected number of collision Scheduler (MES) is developed by exploiting the results of bound analysis. It is shown that, in case one of the cells can acquire knowledge about the reserved resources of the neighboring cell, MES can be implemented by organizing resources of a stack form in a random manner. With the aid of MES, bound expressions are extended by appropriately quantifying absolute uncertainty and certainty conditions in such a way that the amount of knowledge acquired is also included.

Third, considering the practical cases which impose restrictions on schedulers in terms of computational power and time along with persistent scheduling schemes proposed for voice traffic, impacts of prolonged scheduling periods on performances of schedulers are investigated. It is shown that prolonged scheduling periods cause compression and saturation effects. Prolonged scheduling period is also included into the analysis in order to generalize bound expressions.

The paper is organized as follows. Section 2 provides the details of the system model along with the basic assumptions necessary for the analysis. Section 3 gives the upper and lower bounds on the expected number of collisions for general cases. Based on the results in Section 3, MES is developed and knowledge acquisition is embedded into the analysis in Section 4. Section 5 discusses the effects of the prolonged scheduling period

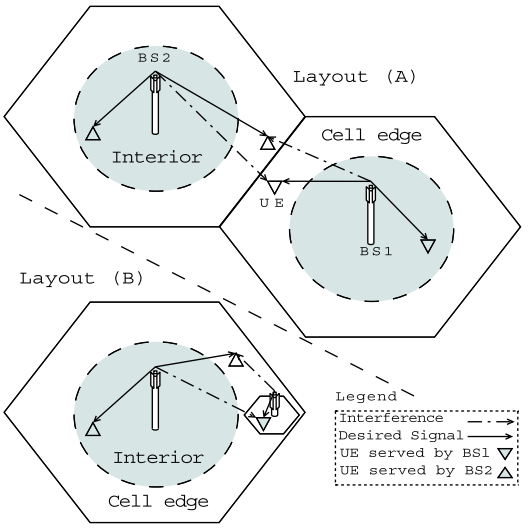

Fig. 1. Two typical two-cell layouts in which cells are assumed to operate under FRO regime along with the "interior/cell edge" distinction. In "Layout (A)", a regular scenario is illustrated where both cells are partially interfered with each other, whereas in "Layout (B)", one of the cells is completely interfered by the other one.

on performance. Numerical results along with relevant discussions are presented in Section 6. Finally, key findings are summarized and future directions are provided in Section 7.

2. System model and basic assumptions

A typical two-cell scenario consists of two interfering cells, which may not necessarily be identical, namely C_c with $c = 1, 2$, under FRO regime. Users in cth cell is denoted with U_c which contains $\mathcal{U}_c$ UEs in it. Each cell C_c performs the interior and cell edge distinction process for each, say jth, UE denoted with u_{cj}. Interior/cell edge distinction is achieved through the use of a specialized function: $\Theta(\cdot)$. For any u_{cj}, $\Theta\left(u_{cj}\right) = 0$ states that UE of interest is an interior user, whereas $\Theta\left(u_{cj}\right) = 1$ represents a cell edge user.[1] Such a scenario is depicted in Fig. 1 with two example layouts. Under FRO regime with no intra-cell interference assumption, $\Theta(\cdot)$ limits interference to cell edge region in which solely ICI takes place. FRO is employed with the common subcarrier[2] set F which contains $\mathcal{F}$ resource elements in it. Once $\Theta(\cdot)$ is applied, each C_c determines $F_c^{(I)}$ for its cell edge users by selecting $\mathcal{F}_c$ elements among F. This model makes no assumption for the distribution of the users across cells. In conjunction with $\Theta(\cdot)$, more general scenarios in which all of the UEs in one of the cells are interfered by some of the UEs in a larger size cell can also be investigated with this way.

All of the UEs in cells are assumed to carry voice traffic whose samples come from a negative exponentially decaying probability density function (PDF) with a decaying rate of λ_H which is the reciprocal of the average holding time μ_H. Stemming from general characteristics of voice traffic, single resource assignment per user is assumed. Assignments are performed at the beginning of each scheduling period T_c for the cell C_c. In order to formalize and later on generalize the problem, C_1 is selected as pilot, whereas C_2 is considered to be an independent cell. Pilot cell is the one on which parameters will be adjusted and their effects are investigated. With this simplification, the behavior of schedulers can be analyzed and easily expanded to general cases such as having a pilot cell surrounded by many interfering cells.

Throughout the analysis no handoff (handover) is assumed to take place in order to make sure of the stability of analysis. However, pure birth process for arrivals (*i.e.*, Poisson process) is considered for each C_c with an average arrival rate of $\lambda_A^{(c)}$. In addition, if no resource is found for any arrival during T_c, then that arrival is assumed to be blocked. If any user releases any of the resources during T_c, it is assumed that those resources cannot be assigned until the next scheduling time.

Scheduling period T_c carries a great importance for ICI management process. Therefore, further details of T_c are essential for analysis. Let T_c be defined in terms of μ_H. This is a reasonable approach, since μ_H is the only parameter in hand providing information about the duration of resource use. Let T_c be expressed in terms of number of scheduling operations as $T_c = \mu_H/\omega_c$. Note that ω_c with $\omega_c \in \mathbb{Z}^+$ provides a better perspective for the scheduling problem due to the following two reasons: First, many communication systems are based on discrete characteristics. For instance, most of the definitions in 3GLTE, which is an OFDMA-based system, are built on a notion called transmission time interval (TTI), which is of discrete nature. Second, scheduling process itself is of discrete nature: for a given "unit period of time" either scheduling is performed or not. Thus, $\omega_c \in \mathbb{Z}^+$ provides a suitable approach for the analysis. Bounds are derived for the pilot cell under the assumption that $T_1 = 1T_\Delta$, which corresponds to maximum number of scheduling operation where T_Δ denotes the minimum period of time in which only one scheduling operation can be performed. Because pure birth process is assumed, system keeps evolving throughout T_1 due to the arrivals. Traffic load is used for quantifying evolution of the system during any scheduling period T and expressed as:

$$r_c = \frac{\lambda_A^{(c)} T}{\mathcal{F}_c}. \tag{1}$$

In (1), it is clear that $r_c \in (0, \infty)$ for $1 \leq \mathcal{F}_c$. However, cases where $1 < r_c$ can be ignored because of blocking assumption made previously; furthermore, blocked arrivals do not have any impact on performance, because no queue or any other facility is assumed in this scenario.

The building blocks of an OFDMA system are subcarriers; therefore, one of the simplest ways of quantifying ICI is to count the number of collisions occurred when scheduling is performed. This requires a formal definition of resource collisions.

[1] Here, $\Theta(\cdot)$ can be any method or a combination of several methods. Reference signal received power (RSRP) measurements with several thresholds in Third Generation Long Term Evolution (3GLTE) [18] can be considered as an instance of $\Theta(\cdot)$.

[2] From this point on, the terms resource and subcarrier are used interchangeably within the text.

Definition 1 (*Resource Collision*)**.** If $W_t = u_{ai}(t) \cap u_{bj}(t)$ and $W_t \neq \emptyset$ for $i = 1, 2, \ldots, \mathcal{U}_a$ and $j = 1, 2, \ldots, \mathcal{U}_b$, then it is said that $\mathcal{W}_t$ "resource collision" occurs where $u_{ai}(t)$ and $u_{bj}(t)$ denote the set of resources used by u_{ai} and u_{bj} at instant t, respectively, and $\mathcal{W}_t$ is the cardinality of W_t.

Even though Definition 1 postulates a way of quantifying resource collisions, it is not very suitable for characterizing an overall behavior of a dynamic system which exhibits stochastic behaviors. This arises from Definition 1 focusing on instantaneous values of collisions. Furthermore, persistent scheduling is considered for voice traffic in order to reduce over-the-air signaling in NGWNs [19]. Resources are assigned UEs and the assignment is maintained for some time in persistent scheduling schemes. From this point of view, it is more reasonable to count collisions per assignment than to count each individual collision occurred for the same assignment when each packet is transmitted, since the latter introduces redundancy. Therefore, expected number of collisions based on Definition 1 will be used in the analysis. In conjunction with the pilot cell approach, persistent scheduling is adopted with $\omega_2 = 1$.

3. Upper and lower bound of expected number of collisions

Upper bound for expected number of collisions expresses the theoretical limit of performance of schedulers operating in a system such as described in Section 2. Different upper bounds can be defined for different strategies. However, if knowledge acquisition about resources in the neighboring cell is taken into account, then it is evident that the upper bound is driven by the absence of knowledge, because schedulers exploit knowledge to reduce the number of collisions.[3]

In this sequel, it is worth mentioning how knowledge can be acquired in such a system. Knowledge is acquired by the following two methods: (E1) information exchange between schedulers and (E2) measurements such as spectrum sensing. The main distinction between these methods is that (E1) requires a backhaul to exchange information, whereas (E2) does not require any backhaul and relies on unilateral effort. It must also be stated that (E1) is more reliable[4] compared to (E2), since measurements might not be very accurate.

In the absence of knowledge, both cells are assumed to reserve their resources among F randomly. Therefore, probability mass function (PMF) of number of collisions is required in order to continue the analysis.[5]

Proposition 3.1 (*PMF of Number of Collisions*)**.** *Given that $\mathcal{F}_1$ and $\mathcal{F}_2$ resources are randomly chosen to be assigned cell edges of C_1 and C_2, respectively, among non-empty set of resources F with $\mathcal{F} \ll \infty$, then the probability mass function of random variable* **K** *representing number of collisions is defined by a hypergeometric distribution that is expressed as:*

$$\Pr(\mathbf{K} = k) = p(k) = \frac{1}{\binom{\mathcal{F}}{\max(\mathcal{F}_1, \mathcal{F}_2)}} \binom{\mathcal{F} - \min(\mathcal{F}_1, \mathcal{F}_2)}{\max(\mathcal{F}_1, \mathcal{F}_2) - k} \times \binom{\min(\mathcal{F}_1, \mathcal{F}_2)}{k}, \quad (2)$$

where k denotes number collisions with $k \in \mathbb{Z}^+$ in $[0, \min(\mathcal{F}_1, \mathcal{F}_2)]$.

Proof. See Appendix A. □

Since PMF is in hand, any statistics desired can be derived. As will be shown subsequently, (2) actually contains the following two important properties: (a) expected number of collisions and (b) breaking point of collisions. It is clear that (a) is related to the upper bound and calculated by the statistical expectation operator (*i.e.*, $E\{\mathbf{K}\}$). Ergo, no extra explanation is required here. As opposed to (a), (b) is related to the lower bound and needs more detailed investigation. First, (a) is analyzed with the following.

Corollary 3.1 (*Expected Number of Collisions of (2)*)**.** *Expected number of collisions of (2) is:*

$$\mathfrak{S} = \frac{\mathcal{F}_1 \mathcal{F}_2}{\mathcal{F}}. \quad (3)$$

Proof. See Appendix B. □

Observe that Corollary 3.1 provides a constant value for expected number of collisions by disregarding the evolution of the system. However, collision does not occur unless reserved resources are assigned. This requires Corollary 3.1 to be extended in terms of traffic loads as follows:

Corollary 3.2 (*Upper Bound*)**.** *Upper bound of expected number of collisions for minimum scheduling period is defined in terms of traffic load r_1 and r_2 by the following:*

$$\mathfrak{U} = r_1 r_2 \mathfrak{S}. \quad (4)$$

In contrast to upper bound, lower bound needs to be considered in the presence of knowledge due to the following reasoning: Definition 1 explicitly states that number of collisions cannot be lower than zero. Therefore, zero collision is a very important characteristic of lower bound. However, it cannot be achieved unless one of the cells is aware of the reservation of its neighbor, because

[3] At this point, one might raise a philosophical objection to this statement by claiming that the upper bound of number of collisions is limited to $\min(\mathcal{F}_c)$ when knowledge acquisition is possible as follows: Number of collisions is maximized when C_1 "imitates" C_2 (*i.e.*, C_1 attains the perfect knowledge about the reservation set of C_2 and follows exactly C_2) or vice versa; therefore, its value is $\min(\mathcal{F}_c)$. Although this claim seems to be true from the algebraic point of view, it is misleading, because every scheduler strives to minimize the expected number of collisions not to maximize it, since interference is mutually detrimental. For $1 < \mathcal{F}$, statistically, it is almost impossible that C_1 "imitates" C_2 unless C_1 acquires the perfect knowledge of the resource use of C_2. $\mathcal{F} = 1$ is the only state in which C_1 can exactly "know" what C_2 does without requirement of any knowledge acquisition. However, this state should be regarded as trivial case, since "assignment" has no meaning in this aspect.

[4] Here, "reliability" refers to the exactitude of the knowledge. However, for the sake of completeness, it must be emphasized that reliability of (E1) actually implies very short delays in the backhaul communications. In this sense, longer delays in (E1) might lead to unreliable results as well.

[5] As expressed in Definition 1, collision is of discrete nature. This gives rise to the use of PMF rather than PDF in the analysis.

cells suppose that reservation sets are chosen randomly among F in the absence of knowledge, as assumed in Proposition 3.1. With the same token in Footnote 3, C_1 can achieve zero collision if and only if it attains the perfect knowledge about the reserved set of C_2 (or vice versa).

In this sequel, the PMF in (2) should be related with zero collision notion in a formal way. In order to achieve this, first the following mathematical tool is defined.

Definition 2 (*Breaking Point*)**.** A breaking point k_ϵ of a precision ϵ is a non-zero number of collisions defined in (2) and satisfies $\Pr(\mathbf{K} \leq k_\epsilon) \leq L < \Pr(\mathbf{K} \leq k_\epsilon + 1)$ where L is a pre-defined certainty with $L \in [\Pr(\mathbf{K} = 0), 1)$ and $\epsilon = 1 - L$.[6]

Although Definition 2 outlines how the breaking point tool is constructed, its existence and uniqueness should also be verified before continuing the analysis.

Corollary 3.3 (*Existence and Uniqueness of Breaking Point*)**.** *There always exists a unique breaking point in (2) for a specified L.*

Proof. See Appendix C. □

Definition 2 and Corollary 3.3 are followed by the identification of unique regions in (2).

Definition 3 (*Vulnerable and Secure Zone*)**.** Vulnerable zone is a unique region within (2) satisfying $k \leq k_\epsilon$, whereas secure zone is its complementary part satisfying $k_\epsilon < k$.

At this point, it is worthwhile to see how PMF in (2) looks like for a general scenario in order both to grasp Definitions 2 and 3 and to have an insight into further steps of analysis, especially for investigating (b). Consider the PMF given in Fig. 2. Visually, it is clear that within right hand side of the vertical dashed line (which is referred to as "secure zone" in Fig. 2), there is no point that provides a significant probability value in contrast to those in left hand side of it. Bearing Definition 2 in mind, assume that one wants to design a system with a precision of $\epsilon = 10^{-6}$. In this case, the separator (*i.e.*, vertical dashed line) should be located on the point where $\Pr(\mathbf{K} \leq k_\epsilon) \leq 1 - \epsilon < \Pr(\mathbf{K} \leq k_\epsilon + 1)$. For the case plotted in Fig. 2, $k_\epsilon = 26$ satisfies this condition by corresponding to a precision of $\epsilon = 8.188 \times 10^{-7}$. This implies that for the point on which the separator is located, with the given settings, it is unlikely that the number of collisions exceed 26. Conversely, with the same settings given, it is very likely to have 26 or less number of collisions.

The discussion related to Fig. 2 points out that there is a strong connection between L (or equivalently ϵ) and zero collisions. In order to elucidate this connection, consider two identical systems one of whose design might regard $E\{\mathbf{K}\}$ as zero for ϵ_1, whereas that of other one might treat $E\{\mathbf{K}\}$ as zero for ϵ_2 where $\epsilon_1 \neq \epsilon_2$. For these two systems, ϵ_1 and ϵ_2 values are the design parameters which

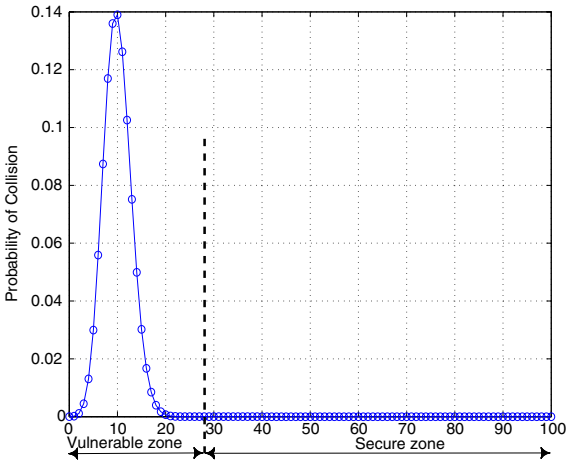

Fig. 2. An example PMF for $\mathcal{F} = 1000$, $\mathcal{F}_1 = \mathcal{F}_2 = \mathcal{F}_z = 100$. The vertical dashed line, which corresponds to a breaking point k_ϵ of a precision ϵ, splits the PMF into two zones which are labeled "vulnerable" and "secure", respectively..

determine zero collision limits. Consequently, breaking point cannot be used for formalizing the theoretical lower bound, since different ϵ values imply different k_ϵs. In order to find a way through this problem, limiting case of breaking points will be examined in what follows.

Consider how breaking point evolves in terms of increasing certainty level, (*i.e.*, $L \to 1$). Before proceeding further, first recall that Definition 2 stipulates $\Pr(\mathbf{K} \leq k_\epsilon) \leq L < \Pr(\mathbf{K} \leq k_\epsilon + 1)$. In the limiting case of L, $k_\epsilon + 1$ diminishes due to the second axiom of probability (*i.e.*, axiom of unit measure). Recall also that Corollary 3.3 guarantees the existence of a unique k_ϵ. However, limiting case does not allow one to find $k_\epsilon + 1$ but k_ϵ. Therefore, the inequality in Definition 2 is forced to degenerate into $\Pr(\mathbf{K} \leq k_\epsilon) = 1$, which also implies $k_\epsilon = \min(\mathcal{F}_1, \mathcal{F}_2)$. With the same token, limiting case leads to $p(k) = \delta(k - k_\epsilon)$ where $\delta(\cdot)$ is the Dirac delta function; therefore, $E\{\mathbf{K}\} = k_\epsilon$.[7] All of the aforementioned statements can succinctly be stated in a formal way as $\lim_{\epsilon \to 0} k_\epsilon = E\{\mathbf{K}\}$. If $E\{\mathbf{K}\}$ is denoted in terms of $\mathcal{F}_c$, it follows

$$\lim_{\epsilon \to 0} k_\epsilon = \frac{\min(\mathcal{F}_1, \mathcal{F}_2) \max(\mathcal{F}_1, \mathcal{F}_2)}{\mathcal{F}}, \tag{5}$$

which is the same as (B.5) in Appendix B. Thus, limiting case reveals a completely new characteristic, because it annihilates the secure zone in Definition 3 and yields the following concept.

Corollary 3.4 (*Bending Point*)**.** *Bending point is the limiting case of any k_ϵ and it represents a constant number of resources given by:*

$$H_k = \min(\mathcal{F}_1, \mathcal{F}_2) \left(1 - \frac{\max(\mathcal{F}_1, \mathcal{F}_2)}{\mathcal{F}}\right). \tag{6}$$

[6] Note that $\Pr(\mathbf{K} = 0)$ corresponds to the probability of having no collisions, which is the same as $p(0)$ in (2).

[7] Existence of breaking point of a PMF under limiting conditions mandates that PMF can be of no other form but of $\delta(\cdot)$. In conformity with this limiting case, $\delta(\cdot)$ represents "absolute certainty" rather than what a usual PMF (or PDF) does. In addition, $\delta(\cdot)$ is the only PMF (or PDF) that has single non-zero probability value due to the axiom of unit measure.

When Definition 2 and Corollary 3.4 are considered together, it is not difficult to see that for the same settings there might be different k_{ϵ_i}s for each ϵ_i level, whereas H_k is a unique value to which each k_{ϵ_i} is asymptotic. From this point of view, bending point is the unique limit of ensemble of all possible breaking points of different certainty levels; therefore, it can safely be used for defining the lower bound.

As stated earlier, bending point actually corresponds to the state in which secure zone is annihilated. This state can best be explained in terms of evolution of system under pure birth process assumption. The system exploits the knowledge acquired to attain zero collision; however, due to arrivals, it reaches such a particular state in which the knowledge acquired is not helpful anymore. This state is the equivalent of absence of knowledge described earlier. Hence, ideally, expected number of collisions should behave according to Corollary 3.2 beyond the bending point. Since ideal case refers to certainty which is of asymptotic nature (*i.e.*, a breaking point with $L \to 1$ or $\lim_{\epsilon\to 0} k_\epsilon$), $E\{\mathbf{K}\}$ is asymptotic to (4) as well. The lower bound of expected number of collisions is then given by the following piecewise-defined asymptote:

$$\mathfrak{L} = \begin{cases} 0, & r_1 \le r_1^{\mathfrak{L}} \quad \text{(a)} \\ \dfrac{\mathfrak{X}}{1 - r_1^{\mathfrak{L}}} \left(r_1 - r_1^{\mathfrak{L}}\right), & \text{otherwise} \quad \text{(b)} \end{cases} \tag{7}$$

where $r_1^{\mathfrak{L}}$ is the bending traffic load of pilot cell and expressed as:

$$r_1^{\mathfrak{L}} = \frac{H_k}{\min\left(\mathcal{F}_1, \mathcal{F}_2\right)}, \tag{8}$$

and $\mathfrak{X}$ denotes the constant part of $\mathfrak{U}$ when pilot cell approach is employed and given by

$$\mathfrak{X} = r_2 \mathfrak{S}.$$

4. MES and its performance

In this section, MES is developed based on the results presented in Section 3. With the aid of MES, it is also shown that (7) can be generalized by including the amount of knowledge acquired into the analysis. The principles of MES is introduced under perfect knowledge case. Generalization of (7) is carried out while imperfect knowledge is discussed.

4.1. MES and its performance in the presence of perfect knowledge

Perfect knowledge refers to a state in which C_1 is assumed to know $F_2^{(I)}$ completely. In such a state, (7a) is attained if and only if the pilot scheduler does not assign the intersecting resources (*e.g.*, set W_t in the sense of Definition 1). Avoiding assigning the intersecting resources is not desired, because it causes underutilization. Therefore, the best strategy for the pilot scheduler is to avoid assigning the intersecting resources unless their assignments are inevitable due to high traffic load. Such a strategy can be performed by assigning the resources

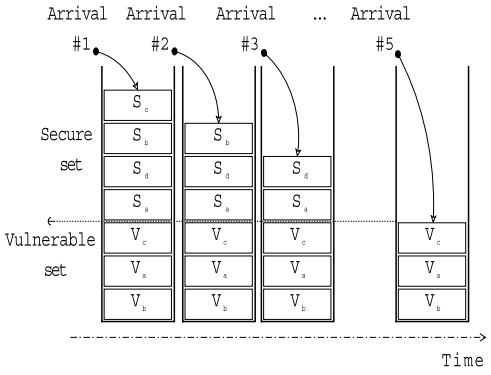

Fig. 3. Illustration of how MES organizes its resources of a stack form and how it performs under incoming arrivals.

of a stack form (*i.e.*, of a first-in-last-out (FILO) scheme). Assume that C_1 splits $F_1^{(I)}$ into two by identifying the "vulnerable" resources via the knowledge acquired about reservation of C_2 with $V = F_1^{(I)} \bigcap F_2^{(I)}$. In order for C_1 to form a stack of resources, V is placed first into the stack (*i.e.*, planned to assign last) as illustrated in Fig. 3. This way, C_1 makes sure that in order for a collision to occur, there must be $\mathcal{F}_1 - \mathcal{V}$ arrivals at least within T_1, where $\mathcal{V}$ is the cardinality of set V. Note that, in the presence of perfect knowledge about $F_2^{(I)}$, this scheme yields the minimum number of collisions, since $\mathcal{V}$ can be regarded as a breaking point. Therefore, MES deviates from zero at $r_1^{\epsilon} = 1 - \mathcal{V}/\mathcal{F}_1$. As Section 3 points out, beyond r_1^{ϵ}, $E\{\mathbf{K}\}$ keeps increasing due to the FILO scheme adopted. However, once $r_1^{\mathfrak{L}}$ is exceeded, $E\{\mathbf{K}\}$ escalates asymptotic to (7b).

4.2. Performance of MES in the presence of imperfect knowledge [Generalized case]

Imperfect knowledge refers to the state where C_1 is assumed to know V partially. Let partial V be denoted as $V_{\mathbf{p}}$ which satisfies $V_{\mathbf{p}} \subseteq V$ with a cardinality of $\mathcal{V}_{\mathbf{p}} \le \mathcal{V}$. Partial knowledge asserts that there are $\mathcal{G} = \mathcal{V} - \mathcal{V}_{\mathbf{p}}$ resources leaked into the secure set from vulnerable set within the stack structure. In other words, if collision occurs in such a scenario, it will definitely be caused by $\mathcal{G}$ resources in the secure set. In order to evaluate the impact of this leakage, assume that pilot cell C_1 performs (E2) with a success rate of $\mathfrak{s}$ where $\mathfrak{s} \in [0, 1]$ yielding $\mathcal{V}_{\mathbf{p}} = \mathfrak{s}\mathcal{V}$. Thus, $\mathcal{G}$ is defined in terms of $\mathfrak{s}$ as $\mathcal{G} = (1 - \mathfrak{s})\,\mathcal{V}$. As indicated in (7), the behavior of MES needs to be investigated based on H_k. In conjunction with (7) and (8), first consider the case where $H_k \neq 0$ and $r_1 \le r_1^{\mathfrak{L}}$. Since probable collisions emanated from $\mathcal{G}$ resources leaked into the secure set, for MES, $E\{\mathbf{K}\}$ actually corresponds to $E\{\mathcal{G}\}$, which is equal to $(1 - \mathfrak{s})\,E\{\mathcal{V}\}$. Observe that $E\{\mathcal{G}\}$ is a scaled version of $E\{\mathcal{V}\}$ due to the initial condition $r_1 \le r_1^{\mathfrak{L}}$ and $E\{\mathcal{V}\}$ is the equivalent of (3) when all of the resources are assigned. Thus, with the aid of (4), it is found that $E\{\mathcal{G}\} = (1 - \mathfrak{s})\,\mathfrak{X} r_1$. In Section 3, it is stated that once bending point is reached, expected number of collisions behaves as though no knowledge acquisition regime (*i.e.*, absence of knowledge) is employed.

Therefore, $\mathfrak{s}$ looses its significance and $E\{\mathfrak{g}\}$ will be asymptotic to (7b) beyond bending point. Performance of MES reveals that (7) can actually be generalized in such a way that $\mathfrak{L}$ includes the amount of knowledge acquired as follows:

$$\mathfrak{L} = \begin{cases} (1-\mathfrak{s})\,\mathfrak{X} r_1, & r_1 \le r_1^{\mathfrak{L}} \quad \text{(a)} \\ \dfrac{\mathfrak{X}}{1-r_1^{\mathfrak{L}}}\left(r_1 - r_1^{\mathfrak{L}}\right), & \text{otherwise.} \quad \text{(b)} \end{cases} \tag{9}$$

In (9), it is indicated that the behavior of $\mathfrak{L}$ might be changed by introducing knowledge acquisition into the system when $r_1 \le r_1^{\mathfrak{L}}$, whereas it does not change when $r_1^{\mathfrak{L}} < r_1$, since (7b) and (9b) are the same. This is not surprising, because bending point is such a point beyond which the presence of knowledge does not have any effect under any circumstances, as mentioned earlier (*i.e.*, annihilation of secure zone).

5. Impacts of scheduling period and generalized bound

Practical cases involve less frequent scheduling, since scheduling is an expensive process in terms of computational power and time. Less frequent scheduling (*i.e.*, $T_\Delta < T_1$) has the following two impacts on performance: compression and saturation. These two effects are analyzed below.

5.1. Compression effect

When scheduling period T_1 is prolonged while all of the other parameters are constant, the most important change occurs in evolution of the system due to pure birth process assumption. In order to identify the behavior in a normalized way, as in previous sections, pilot cell traffic approach will be used. Assume that a new scheduling period is adopted by C_1 as $T_1^{\text{new}} = nT_\Delta$ with $1 < n$ and $n \in \mathbb{R}^+$. The new traffic loads in both cells for the period calculated become $r_c^{\text{new}} = \lambda_A^{(c)} n T_\Delta / \mathcal{F}_c$. If this is combined with (1) for $T = T_\Delta$, it yields $r_c^{\text{new}} = n r_c$. The most striking consequence of r_c^{new} is that the behavior of bounds remains the same, but it is compressed into $r_1' \in \left(0, 1/n^2\right]$ where r_1' represents the transformed version of r_1, which is again defined within the unit interval by preserving $\lambda_A^{(1)}$ $\left(\text{i.e., } r_1' \in (0,1]\right)$ with $r_1' = \lambda_A^{(1)} T_\Delta / \mathcal{F}_1$.[8] Note that although T_1 is prolonged by a factor of n, compression occurs within $\left(0, 1/n^2\right]$. This stems from r_c^{new}, because prolonged period affects both of the cells simultaneously. In order to see this, Corollary 3.2 can be examined. Since r_1' is assumed to be the only independent variable, $\mathfrak{U}$ is rewritten in terms of r_c^{new} yielding:

$$\mathfrak{U}^{\text{new}} = r_1^{\text{new}} r_2^{\text{new}} \mathfrak{S} = \left(n r_1'\right)(n r_2)\,\mathfrak{S} = n^2 \mathfrak{X} r_1'. \tag{10}$$

Observe that $\mathfrak{U}$ for $r_1 \in (0,1]$ is the same as $\mathfrak{U}^{\text{new}}$ for $r_1' \in \left(0, 1/n^2\right]$, which is the evidence of compression effect at a rate of n.

[8] Such a transformation is necessary from the perspective of analysis, because arrival rate is an independent process whose parameter $\lambda_A^{(c)}$ cannot be changed by the system. Therefore, when T_1^{new} is adopted for the pilot cell approach, $r_1' \in (0,1]$ is required in order to evaluate the behavior of the system in a comparative way.

5.2. Saturation effect

Despite (10) provides the precise behavior of $\mathfrak{U}^{\text{new}}$, one might wonder if (3) is violated by a particular n value. For instance, some n satisfying $\frac{1}{r_2} < n$ actually seems to cause (10) to exceed $\mathfrak{S}$ for $\frac{1}{n} < r'$. This concern is already cleared by the domain of k in Proposition 3.1. Nonetheless, (10) should be rewritten in the following form in order to avoid any confusions:

$$\mathfrak{U}^{\text{new}} = \left(n r_1'\right) \min\left(n r_2, 1\right) \mathfrak{S} = n \mathfrak{S}_{\min} r_1', \tag{11}$$

where $\mathfrak{S}_{\min} = \min(n\mathfrak{X}, \mathfrak{S})$. To proceed further, let the remaining $r_1' \in \left(1/n^2, 1\right]$ interval be decomposed into the following two subintervals: $r_1' \in \left(1/n^2, 1/n\right]$ and $r_1' \in (1/n, 1]$. Because C_1 can still accept new arrivals within $\left(1/n^2, 1/n\right]$ and r_2 is assumed to be constant, $E\{\mathbf{K}\}$ increases with the same rate, that is $n \min(n r_2 \mathfrak{S}, \mathfrak{S})$, due to the same reasons provided for (11). When the last subinterval $(1/n, 1]$ is considered, $\frac{1}{n} < r_1'$ implies that C_1 runs out of resources and further arrivals do not affect the number of collisions due to blocking assumption; therefore, $E\{\mathbf{K}\}$ remains constant at $\mathfrak{U}^{\text{new}} = \mathfrak{S}_{\min}$. Note that $\mathfrak{U}^{\text{new}}$ equals $n\mathfrak{X}$ for $r_2 \le 1/n$, whereas it equals $\mathfrak{S}$ for $1/n < r_2 \le 1$, which verifies that any $T_\Delta < T_1$ gives rise to saturation, if all of the other parameters are assumed to remain the same in the system.

Compression and saturation effects can be combined to generalize the bound expressions. From (4) and (9a), it is clear that the only difference between upper and lower bound is the knowledge acquisition where upper bound represents the absence of knowledge. As will be shown subsequently, knowledge acquisition allows one to unify the lower and upper bounds, whereas prolonged scheduling period allows (9) to be generalized. Since (8) is already defined in terms of traffic load, $\mathfrak{L}$ can be expressed in terms of $\mathfrak{s}$ and n with the aid of (9) as follows:

$$\mathfrak{L}' = \begin{cases} n\mathfrak{S}_{\min}(1-\mathfrak{s})\, r_1', & 0 < r_1' \le \dfrac{r_1^{\mathfrak{L}}}{n} \quad \text{(a)} \\ \dfrac{n\mathfrak{S}_{\min}}{1-r_1^{\mathfrak{L}}}\left(r_1' - \dfrac{r_1^{\mathfrak{L}}}{n}\right), & \dfrac{r_1^{\mathfrak{L}}}{n} < r_1' < \dfrac{1}{n} \quad \text{(b)} \\ \mathfrak{S}_{\min}, & \dfrac{1}{n} < r_1' \le 1 \quad \text{(c)} \end{cases} \tag{12}$$

There are two important facts regarding (12). First, compression and saturation effects form a pattern in both upper and lower bounds. It can be seen in (11) for upper bound and (12) for lower bound that they include $n\mathfrak{S}_{\min}$ and $\mathfrak{S}_{\min}$ for compression and saturation effects, respectively. Second, for $\mathfrak{s} < 1$ and $1 < n$, (12a) provides larger asymptotic values compared to (12b) when r_1' is in the vicinity of $r_1^{\mathfrak{L}}/n$. This can be verified by applying $r_1' = r_1^{\mathfrak{L}}/n$ and $r_1' = r_1^{\mathfrak{L}}/n + \xi$ in (12a) and (12b), respectively, where ξ is infinitesimal. Since both (12a) and (12b) are slants with particular slopes, intersection point of these two slants can be used for purifying the intervals of (12) even though they actually do not intersect due to intervals in which they are defined. This way, $\mathfrak{L}'$ can be redefined in

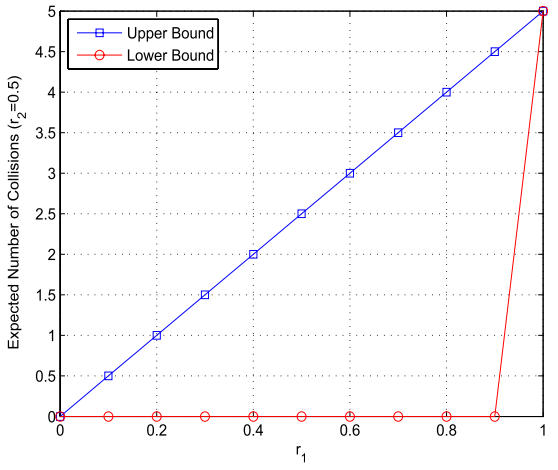

Fig. 4. An example plot of both upper and lower bounds for $\mathcal{F} = 1000$, $\mathcal{F}_1 = \mathcal{F}_2 = 100$, and a fixed traffic load in C_2 with $r_2 = 0.5$. Upper bound follows a slant which is defined in (4), whereas lower bound is a piecewise-defined function that is based on bending point given in (8) and found to be $r_1^{\mathfrak{C}} = 0.9$ here.

a more concise way as follows:

$$\mathfrak{L}' = \begin{cases} n\,(1-\mathfrak{s})\,\mathfrak{S}_{\min} r_1', & 0 < r_1' \le r' \quad \text{(a)} \\ \dfrac{n\mathfrak{S}_{\min}}{1-r_1^{\mathfrak{C}}}\left(r_1' - \dfrac{r_1^{\mathfrak{C}}}{n}\right), & r' < r_1' \le \dfrac{1}{n} \quad \text{(b)} \\ \mathfrak{S}_{\min}, & \dfrac{1}{n} < r_1' \le 1 \quad \text{(c)} \end{cases} \tag{13}$$

where r' is the intersection point of the slants in (12a) and (12b), and it is found to be:

$$r' = \frac{r_1^{\mathfrak{C}}}{n\left(\mathfrak{s} + r_1^{\mathfrak{C}} - \mathfrak{s} r_1^{\mathfrak{C}}\right)}. \tag{14}$$

Observe that r' is the translated (or generalized) version of $r_1^{\mathfrak{C}}$ in the presence of both $\mathfrak{s}$ and n. It is also easy to verify that (13) along with (14) encompasses (4), (7), and (9) with appropriate $\mathfrak{s}$ and n values.

6. Numerical results

In the simulations, FRO regime is employed with $\mathcal{F} = 1000$ resources and $\mathcal{F}_1 = \mathcal{F}_2 = \mathcal{F}_z = 100$. Each simulation setup is run 10 000 times in order to obtain reliable statistics. Theoretical bounds are obtained for $T_1 = T_\Delta$ and all of the time related parameters such as μ_H are defined in terms of T_Δ as well. A typical voice encoder period of 20 ms is chosen for T_Δ and $T_2 = \mu_H = 120T_\Delta$, which corresponds approximately to half of the mean talk spurt duration of 5 s (*i.e.* time period of staying in active state in two-state voice activity model) [20]. Each arrival is considered to be assigned single resource. Resource collision is calculated based on Definition 1 for each scheduling period at each step, then $E\{\mathbf{K}\}$ is calculated.

To begin with, upper and lower bounds are plotted in Fig. 4 for $r_2 = 0.5$. As can be seen, upper bound is a slant whose slope is $r_2\mathcal{F}_z^2/\mathcal{F}$, whereas lower bound obeys (13) for $\mathfrak{s} = n = 1$ with $r_1^{\mathfrak{C}} = 0.9$.

In order to see how MES behaves under different scenarios, knowledge acquisition regime is employed in simulations while the previous settings are maintained. The performance of MES for $\mathfrak{s} = 1$ is given in Fig. 5. As described earlier, $\mathfrak{s} = 1$ allows MES to avoid collision by forming its assignment set as a stack. The impact of ϵ and corresponding k_ϵ is seen when $0.8 \le r_1 < r_1^{\mathfrak{C}}$. In Section 3, recall that for the same settings k_ϵ is found to be 26 of a $\epsilon = 10^{-6}$ precision implying $\mathcal{V} = 26$ or $r_1^{\epsilon} = 0.74$. This discrepancy stems from the fact that simulation could not reach the desired accuracy, because it ran only 10^4 times. In order to confirm this, the PMF is reexamined for $\epsilon = 10^{-4}$ and $\mathcal{V}$ is found to be 20, which corresponds to $r_1^{\epsilon} = 0.8$ and confirms the results in Fig. 5.[9] This example sheds light on the reason why the use of bending point is essential for the analysis.

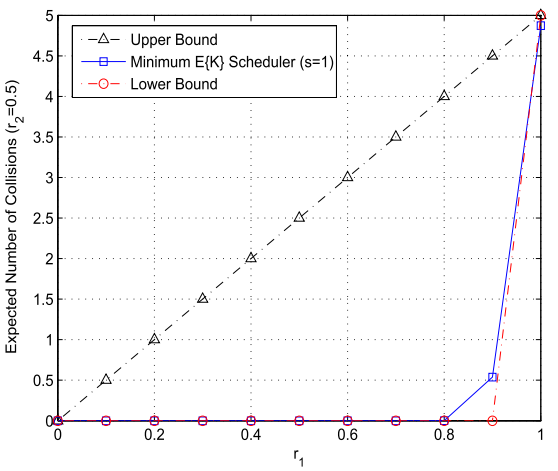

Fig. 5. Performance of MES for $\mathfrak{s} = 1$ delineated by the corresponding upper and lower bounds. Note that MES deviates from zero collision before it reaches the bending point and $E\{\mathbf{K}\}$ escalates asymptotic to (13b) for $n = 1$ beyond bending point.

The impact of knowledge acquisition on the performance of MES is given in Fig. 6 for several scenarios with $\mathfrak{s} \in [0, 1]$. The results are in conformity with (13). For instance, the scheduler with $\mathfrak{s} = 0.5$ and $n = 1$ follows (13a) with a slant whose slope is $\approx$2.78. Again, as in other $\mathfrak{s}$ values, $\mathfrak{s} = 0.5$ is asymptotic to (13b) beyond r', as predicted. Note also that upper bound is attained when $\mathfrak{s} = 0$.

Up until now, $T_1 = T_\Delta$ is considered. In order to see the impact of T_{new}, the performance of MES is plotted in Fig. 7 for $n = 2, 4, 8$ with $r_2 = 0.2$ and $\mathfrak{s} = 0.4$. In Fig. 7, both the compression and saturation effects are clearly seen while $r_1' \to 0$. In order to exemplify how bounds delineate MES, $n = 4$ is chosen. As stated in (13a), lower bound follows a slant whose slope is $n\,(1-\mathfrak{s})\,\mathfrak{S}_{\min} = 19.2$ for $0 < r_1' \le r'$. The performance is upper bounded by a slant whose slope is $n\mathfrak{S}_{\min} = 32$, as given in (11). Note that upper bound can also be obtained by applying $\mathfrak{s} = 0$ in (13a) and (14), respectively. Saturation effect is seen in each realization of n, for $\frac{1}{n} < r'$. Note also that how clipping (*i.e.*, $\mathfrak{S}_{\min}$) takes place for $n = 8$ in $\frac{1}{n} < r'$, because $\frac{1}{r_2} < n$ is satisfied.

[9] The relationship between ϵ and simulated value of breaking point can also be verified from (2) with the same argument presented in Section 3. In (2), $p(k)$ is always greater than zero for all finite values of $\mathcal{F}$. This implies that if one were to run the same simulation for infinite amount of time, there would definitely be a collision even for the case $\mathcal{V} = \min(\mathcal{F}_1, \mathcal{F}_2)$, which corresponds to $r_1^{\epsilon} = 0$.

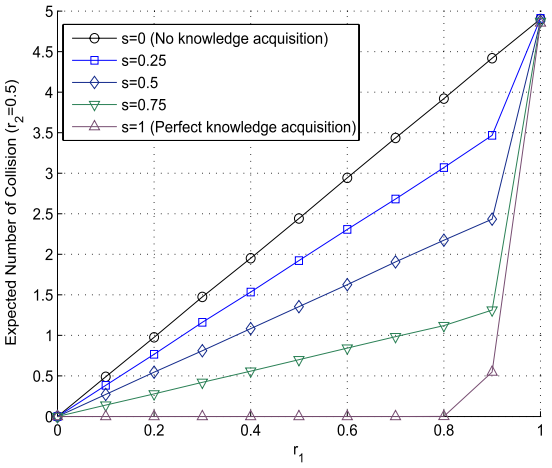

Fig. 6. Performance of MES under different knowledge acquisition scenarios for $s \in [0, 1]$, $\mathcal{F} = 1000$, $\mathcal{F}_1 = \mathcal{F}_2 = 100$, and a fixed traffic load in C_2 with $r_2 = 0.5$.

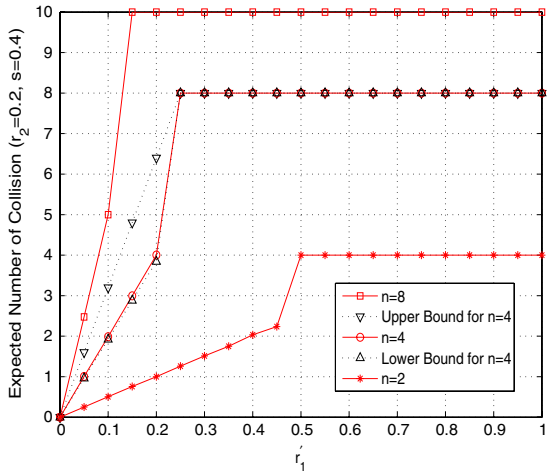

Fig. 7. Performance of MES under three different scheduling periods which are obtained by $n = 2, 4, 8$ for $s = 0.4$, $\mathcal{F} = 1000$, $\mathcal{F}_1 = \mathcal{F}_2 = 100$, and a fixed traffic load $r_2 = 0.2$. Note that the horizontal axis is r_1', which corresponds to the transformed version of r_1, as stated in both (12) and (13).

7. Concluding remarks

In this study, upper and lower bound of scheduler performances for resource collisions in broadband OFDMA-based systems are derived for voice traffic. Under FRO regime, it is shown that upper bound is the expected value of a hypergeometric PMF, whereas lower bound is a piecewise-defined asymptote, which bends at a particular point. It is found that prolonged scheduling periods lead to compression and saturation effects on the performance of schedulers. Hence, analysis is extended in such a way as to generalize the bound expressions in terms of both the knowledge acquired and scheduling period.

Although voice is still considered to be the most dominant traffic type, Internet draws significant attention as well. Exhibiting very different traffic characteristics renders Internet a challenging issue for ICI management. Investigating the performance bounds of schedulers for Internet traffic is of extreme importance for NGWNs. Therefore, derivation of these bounds will help researchers develop better schedulers for different types of traffic.

Acknowledgement

The work of Serhan Yarkan was carried out during an internship at Mitsubishi Electric Research Laboratories (MERL).

Appendix A. Proof of Proposition 3.1

Proof. In the light of Definition 1, it is clear that maximum number of collisions can be $\min(\mathcal{F}_1, \mathcal{F}_2)$. The number of all possible resource assignment pairs is then equal to the number of elements in the Cartesian product of the sets of all available selections in each cell and given by:

$$K_S = \binom{\mathcal{F}}{\min(\mathcal{F}_1, \mathcal{F}_2)} \binom{\mathcal{F}}{\max(\mathcal{F}_1, \mathcal{F}_2)}.$$

Consider the cell whose $\mathcal{F}_c$ is the minimum. In this cell C_c, the number of all possible selections that yields exactly k number of collisions is found as follows: The number of all possible selections within that cell for $\min(\mathcal{F}_1, \mathcal{F}_2)$ is

$$K_1 = \binom{\mathcal{F}}{\min(\mathcal{F}_1, \mathcal{F}_2)}.$$

Among K_1 selections, the number of selections that yields exactly k collisions is given by:

$$K_2 = \binom{\mathcal{F} - \min(\mathcal{F}_1, \mathcal{F}_2)}{\max(\mathcal{F}_1, \mathcal{F}_2) - k}.$$

This stems from the fact that, if $\min(\mathcal{F}_1, \mathcal{F}_2)$ of the resources are reserved among $\mathcal{F}$, then remaining number of resources in the neighboring cell that might cause collision is simply $\mathcal{F} - \min(\mathcal{F}_1, \mathcal{F}_2)$. Among $\mathcal{F} - \min(\mathcal{F}_1, \mathcal{F}_2)$ resources, if exactly k resources are colliding, then k resources can be considered as reserved (since they are colliding, they will be in the selections anyway). This implies that, remaining selections (number of resources) are reduced to $\max(\mathcal{F}_1, \mathcal{F}_2) - k$. Hence, the total number of selections among this set is expressed by K_2. The number of all possible different orderings for k resources causing collisions among $\min(\mathcal{F}_1, \mathcal{F}_2)$ is

$$K_3 = \binom{\min(\mathcal{F}_1, \mathcal{F}_2)}{k}.$$

Since the probability space, namely K_S, is known and the number of all possible selections are defined, the desired PMF can be obtained by

$$p(k) = \frac{K_1 K_2 K_3}{K_S}$$

which is the equivalent of (2) and this completes the proof. □

Appendix B. Proof of Corollary 3.1

Proof. For the sake of brevity in notation, let $\min(\mathcal{F}_1, \mathcal{F}_2) = M_{\min}$ and $\max(\mathcal{F}_1, \mathcal{F}_2) = M_{\max}$. Stemming from the fact that k can take values in the range of $[0, \min(\mathcal{F}_1, \mathcal{F}_2)]$ and PMF in (2) is of discrete nature, statistical expectation is given by $E\{\mathbf{K}\} = \sum_{k=0}^{M_{\min}} k\,p(k)$. If $p(k)$ is replaced with its equivalent in (2) bearing $r\binom{n}{r} = n\binom{n-1}{r}$ in mind, then:

$$E\{\mathbf{K}\} = \frac{M_{\min}}{\binom{\mathcal{F}}{M_{\max}}} \sum_{k=1}^{M_{\min}} \binom{\mathcal{F} - M_{\min}}{M_{\max} - k} \binom{M_{\min} - 1}{k - 1}. \quad \text{(B.1)}$$

If all of the common terms in the summation are regrouped, then it reads:

$$E\{\mathbf{K}\} = \frac{M_{\min}(\mathcal{F} - M_{\min})!}{\binom{\mathcal{F}}{M_{\max}} (M_{\max} - M_{\min})!\,(\mathcal{F} - M_{\max} - M_{\min} + 1)!} \times \sum_{k=1}^{M_{\min}} \frac{\binom{M_{\min}-1}{k-1}}{\prod_{j=k}^{M_{\min}-1} (M_{\max} - j) \prod_{q=2}^{k} (\mathcal{F} - M_{\max} - M_{\min} + q)}. \quad \text{(B.2)}$$

When the denominators in the summation are equalized with appropriate coefficients, (B.2) becomes:

$$E\{\mathbf{K}\} = \frac{M_{\min}(\mathcal{F} - M_{\min})!}{\binom{\mathcal{F}}{M_{\max}} (M_{\max} - M_{\min})!\,(\mathcal{F} - M_{\max} - M_{\min} + 1)!} \times \frac{1}{\prod_{j=1}^{M_{\min}-1} (M_{\max} - j)(\mathcal{F} - M_{\max} - j + 1)} \times \sum_{k=1}^{M_{\min}} \binom{M_{\min} - 1}{k - 1} \underbrace{\prod_{j=2}^{k} (M_{\max} - j + 1)}_{\mathfrak{A}_1} \times \underbrace{\prod_{q=k}^{M_{\min}-1} (\mathcal{F} - M_{\max} - M_{\min} + q + 1)}_{\mathfrak{A}_2}. \quad \text{(B.3)}$$

In (B.3), for a given k, consider sum of first and last terms of products $\mathfrak{A}_1$ and $\mathfrak{A}_2$, respectively (*i.e.*, $j = 2$ and $q = M_{\min} - 1$). If a change of variable is applied for this case with sum of these two terms as $u = \mathcal{F} - 1$, after some mathematical manipulations (B.3) simplifies to:

$$E\{\mathbf{K}\} = \frac{M_{\min}(\mathcal{F} - M_{\min})!}{\binom{\mathcal{F}}{M_{\max}} (M_{\max} - M_{\min})!\,(\mathcal{F} - M_{\max} - M_{\min} + 1)!} \times \frac{\prod_{k=1}^{M_{\min}-1} (u - k + 1)}{\prod_{j=1}^{M_{\min}-1} (M_{\max} - j) \prod_{q=2}^{M_{\min}} (\mathcal{F} - M_{\max} - M_{\min} + q)}. \quad \text{(B.4)}$$

Finally, one can expand all of the factorials and products and simplify (B.4) further to:

$$E\{\mathbf{K}\} = \frac{M_{\min} M_{\max}}{\mathcal{F}}, \quad \text{(B.5)}$$

which conforms with (3) in Corollary 3.1 and completes the proof. □

Appendix C. Proof of Corollary 3.3

Proof. If $\mathbf{K}$ denotes the number of collisions in (2), then, sample space is given by $S = \{0, 1, \ldots, \min(\mathcal{F}_1, \mathcal{F}_2)\}$. For an arbitrary $k \in S$ recall that $\Pr(\mathbf{K} \le k) = \sum_{i=0}^{k} p(i)$, which causes $\Pr(\mathbf{K} \le k)$ to be strictly increasing.[10] Therefore, one is allowed to write $\Pr(\mathbf{K} \le k+1) = \Pr(\mathbf{K} \le k) + p(k+1)$ for all k satisfying $k < \min(\mathcal{F}_1, \mathcal{F}_2)$. The unit measure axiom necessitates $\Pr(\mathbf{K} \le \min(\mathcal{F}_1, \mathcal{F}_2)) = 1$. Note that Definition 2 stipulates $L \in [\Pr(\mathbf{K} = 0), 1)$ and $\Pr(\mathbf{K} \le k)$ can be defined in terms of intervals such as $\Pr(\mathbf{K} \le k) \in [p(0), 1)$ for $0 \le k < \min(\mathcal{F}_1, \mathcal{F}_2)$. Along with the property of being strictly increasing, this causes the set P actually to form a strict order for a given S as $(P, <)$ where:

$$P = \{\Pr(\mathbf{K} \le k) \mid 0 \le k < \min(\mathcal{F}_1, \mathcal{F}_2)\}. \quad \text{(C.1)}$$

Therefore, for any given L satisfying $L \in [\Pr(\mathbf{K} = 0), 1)$, there always exists a unique pair $(k, k+1)$ in P corresponding to k_ϵ and this completes the proof. □

References

[1] T.S. Rappaport, Wireless Communications: Principles and Practice, 2nd ed., in: Prentice Hall Communications Engineering and Emerging Technologies Series, Prentice–Hall, Inc., NJ, USA, 2002.

[2] I. Katzela, M. Naghshineh, Channel assignment schemes for cellular mobile telecommunication systems: a comprehensive survey, IEEE Personal Communications 3 (3) (1996) 10–31 (see also IEEE Wireless Communications).

[3] M. Sternad, T. Svenssony, T. Ottossony, A. Ahlen, A. Svenssony, A. Brunstrom, Towards systems beyond 3G based on adaptive OFDMA transmission, in: Adaptive Transmission, Proceedings of the IEEE 95 (2007) 3472–3477 (special Issue) Invited Paper.

[4] G. Li, H. Liu, Downlink dynamic resource allocation for multi-cell OFDMA system, in: Proceedings of 58th IEEE Vehicular Technology Conference, VTC 2003–Fall, vol. 3, 2003, pp. 1698–1702.

[5] P. Magnusson, J. Lundsjö, J. Sachs, P. Wallentin, Radio resource management distribution in a beyond 3G multi-radio access architecture, in: Proceedings of IEEE Global Telecommunications Conference, GLOBECOM'04, Dallas, TX, USA, vol. 6, 2004, pp. 3472–3477.

[6] R. Bachl, P. Gunreben, S. Das, S. Tatesh, The long term evolution towards a New 3GPP air interface standard, Bell Labs Technical Journal 11 (4) (2007) 25–51.

[7] K. Hooli, J. Lara, S. Pfletschinger, M. Sternad, S. Thilakawardana, Radio resource management architecture for spectrum sharing in B3G systems, in: Proceedings of Wireless World Research Forum Meeting 15, Paris, France, vol. 3, 2005, pp. 1–6.

[8] M.C. Necker, Towards frequency reuse 1 cellular FDM/TDM systems, in: Proceedings of the 9th ACM International Symposium on Modeling Analysis and Simulation of Wireless and Mobile Systems, MSWiM'06, ACM Press, Terromolinos, Spain, 2006, pp. 338–346. http://dx.doi.org/http://doi.acm.org/10.1145/1164717.1164775.

[9] E. Oh, M. gyun Cho, S. Han, C. Woo, D. Hong, Performance analysis of dynamic channel allocation based on reuse partitioning in multi-cell OFDMA uplink systems, IEICE Transactions on Fundamentals E89–A (6) (2006) 1566–1570.

[10] G. Fodor, M. Telek, C. Koutsimanis, Performance analysis of scheduling and interference coordination policies for OFDMA networks, Computer Networks 52 (2008) 1252–1271.

[10] Note that $\Pr(\mathbf{K} \le k)$ is strictly increasing rather than only increasing due to non-zero probabilities for finite $\mathcal{F}$, as stated in Section 3. The only exception for this statement is a PMF (or PDF) of $\delta(\cdot)$ form. This case will not be considered here due to the reasons explained in Footnote 7.

[11] C.T.T. Chahed, Modeling of streaming and elastic flow integration in OFDMA-based IEEE802.16 WiMAX, Computer Networks 30 (2007) 3644–3651.
[12] D.-H. Kim, B.-H. Ryu, C.-G. Kang, Packet scheduling algorithm considering a minimum bit rate for non-realtime traffic in an OFDMA/FDD-based mobile internet access system, ETRI Journal 26 (1) (2004) 48–52.
[13] S.-E. Elayoubi, B. Fourestie, X. Auffret, On the capacity of OFDMA 802.16 systems, in: Proc. IEEE International Conference on Communications, ICC'06, Istanbul, Turkey, vol. 4, 2006, pp. 1760–1765.
[14] X. Kai, T. Xiaofeng, W. Ying, Z. Ping, Inter-cell packet scheduling in ofdma wireless network, in: Proc. IEEE 65th Vehicular Technology Conference, VTC2007-Spring, Dublin, Ireland, 2007, pp. 3115–3119.
[15] T. Kwon, H. Lee, S. Choi, J. Kim, D.-H. Cho, S. Cho, S. Yun, W.-H. Park, K. Kim, Design and implementation of a simulator based on a cross-layer protocol between MAC and PHY layers in a WiBro Compatible IEEE 802.16e OFDMA system, IEEE Communications Magazine 43 (12) (2005) 136–146.
[16] A. Fernekeb, A. Klein, B. Wegmann, K. Dietrich, Influence of traffic models and scheduling on the system capacity of packet-switched mobile radio networks, in: Proc. 15th IST Mobile and Communications Summit, Mykonos, Greece, 2006, pp. 1–5.
[17] H. Lei, X. Zhang, Y. Wang, Real-time traffic scheduling algorithm for MIMO–OFDMA systems, in: Proc. IEEE International Conference on Communications ICC'08, Beijing, China, 2008, pp. 4511–4515.
[18] Ericsson, Physical layer measurement period of UE measurements, Agenda Item 4.6 R4–070407, 3GPP TSG RAN, Sophia Antipolis, France, WG4#42bis, Discussion, Apr. 2–4, 2007.
[19] D. Jiang, H. Wang, E. Malkamaki, E. Tuomaala, Principle and performance of semi-persistent scheduling for VoIP in LTE system, in: Proc. Intl. Conf. on Wireless Comm., Networking & Mobile Comp., Shangai, China, 2007, pp. 2861–2864.
[20] 3GPP, LTE physical layer framework for performance verification, TSG RAN WG1 Meeting #48 R1–070674, 3rd Generation Partnership Project, 3GPP, St. Louis, MI, USA, Decision, Feb. 12–16, 2007.

Serhan Yarkan received his both B.S. and M.Sc. degrees in Computer Science from Istanbul University, Istanbul, Turkiye in 2001 and 2003, respectively. He received his Ph.D. degree in 2009 from Department of Electrical Engineering at the University of South Florida. He is currently with Department of Computer and Electrical Engineering at Texas A & M University, College Station, Texas, as a post-doctoral research associate. His research interests include statistical signal processing, cognitive radio, wireless propagation channel modeling, cross-layer adaptation and optimization, and interference management in next generation wireless networks.

Koon Hoo Teo received his M.Sc. and Ph.D. from University of Alberta in 1985 and 1990, respectively. He was with Nortel for about 15 years where he has worked in wireless system research and product development. For the last five years at Nortel, he worked as a Radio Architect and a System Engineering Manager where he was actively involved in the research and implementation issues of a number of 3G and 4G wireless systems and translated a number of initial research concepts into highly competitive products. The wireless systems he worked in include Wireless Mesh Networks and WiMAX systems. He left Nortel and joined MERL in 2006. His work at MERL includes Cognitive Radio, Game Theory, Wireless Mesh and Multi-Hop Systems. His current research interest includes theory, simulation and characterization of Meta Material and its applications in Energy and Communication space. He is currently a holder of more than 20 US patents and at least another 35 pending. He is also the author and co-author of more than 30 journal and conference papers.

Hüseyin Arslan has received his Ph.D. degree in 1998 from Southern Methodist University, Dallas, TX. From January 1998 to August 2002, he was with the research group of Ericsson Inc., NC, USA. Since August 2002, he has been with Electrical Engineering Dept. of University of South Florida. His research interests are related to advanced signal processing techniques for cross-layer design, networking adaptivity and QoS control for UWB, OFDM-based wireless technologies with emphasis on WiMAX, and cognitive and SDR.

Jinyun Zhang received her Ph.D. degree in electrical engineering from University of Ottawa, Canada in 1991. Dr. Zhang then joined Nortel Networks, where she held various management positions and engineering positions of increasing responsibility in the areas of digital signal processing, wireless communication and optical networks. Since 2001, Dr. Zhang has been the Manager of the Digital Communications & Networking Group at Mitsubishi Electric Research Laboratories (MERL), Cambridge, MA, USA. Currently, she is MERL Fellow and leading various new broadband wireless communications and networking research projects and smart grid research and standardization activities. Dr. Zhang has authored and co-authored more than 140 publications, invented and co-invented more than 130 patents and patent applications, and made numerous contributions to international wireless communications standards. Dr. Zhang is a Fellow of the IEEE and a member of the IEEE AP, BT, COMM, IT, ITS, LEO, SP, and VT Socieites. She serves as an Associate Editor of IEEE Transactions on Broadcasting, an AdCom member of IEEE Broadcasting Technology Society, and has served as a Technical Program Committee member for various IEEE conferences.

Khalid A. Qaraqe (M'97-S'00) was born in Bethlehem. He received the B.S. degree in EE from the University of Technology, Baghdad in 1986, with honors. He received the M.S. degree in EE from the University of Jordan, Jordan, in 1989, and he earned his Ph.D. degree in EE from Texas A & M University, College Station, TX, in 1997. From 1989 to 2004 Dr. Qaraqe has held a variety positions in many companies and he has over 12 years of experience in the telecommunication industry. He has worked for Qualcomm, Enad Design Systems, Cadence Design Systems/Tality Corporation, STC, SBC and Ericsson. He has also worked on numerous GSM, CDMA, WCDMA projects and has experience in product development, design, deployments, testing and integration. Dr. Qaraqe joined the department of Electrical Engineering of Texas A & M University at Qatar, in July 2004, where he is now associate professor. Dr. Qaraqe research interests include communication theory and its application to design and performance, analysis of cellular systems and indoor communication systems. Particular interests are in the development of 3G UMTS, cognitive radio systems, broadband wireless communications and diversity techniques.